Transient mid-ir picosecond spectroscopy of indium arsenide at room temperature: Evidence of spectral hole burning due to nonthermalized carriers

K. L. Vodopyanov* and H. Graener

EP III Universität Bayreuth, Postfach 101251, D-8580 Bayreuth, Federal Republic of Germany

C. C. Phillips

Physics Department, Imperial College, London SW7 2AZ, United Kingdom

Spectral hole burning in the interband absorption continuum of InAs has been studied using pump radiation (with photon energy 32–57 meV above the band edge and intensity $\approx 10^7$ W/cm^2) generated by a picosecond midinfrared double-resonance pump-probe spectrometer. The quasi-steady-state spectral holes observed had depths which followed the instantaneous pump intensity and typical widths of ≈ 300 cm^{-1}. The evolution of the shape of the spectral holes is correlated with the primary carrier scattering processes and an analysis of their widths and depths gives values of the carrier-carrier thermalization and dephasing times $T_1 \approx 65$ fs and $T_2 \approx 40$ fs, respectively.

InAs is a direct-gap semiconductor with a small 300-K optical band gap E_g of 0.35 eV (2825 cm^{-1}, $\lambda = 3.54$ μm) and a large effective-mass ratio between electrons (m_e^*) and heavy holes (m_{hh}^*).[1] A number of nonlinear optical properties of InAs associated with the fundamental band-gap resonance have been studied recently, and have been used successfully for optical switching, optical bistability, optical signal processing, and mid-IR laser intracavity control.[2–6] Absorptive nonlinearities have also been employed to achieve the passive mode locking of an YSGG:Er^{3+} 3-μm laser producing pulse durations of 30 ps and peak output powers of 10^7 MW.[6]

For this study we use the picosecond midinfrared (IR) pump-probe spectroscopy[7] system which was used previously for ≈ 10-psec resolution studies of 0.09–3.3-μm undoped InAs epilayers.[8,9] The Auger coefficient was measured to be 1.1×10^{-26} cm^{6}sec^{-1} and it was also shown that for pump-probe delays $t_D > 15$ psec the carrier occupation probabilities in the conduction and valence bands closely follow Fermi functions with well-defined quasi-Fermi energies and carrier temperatures equal to the 300-K lattice.[8]

The study of InAs transient absorption spectra under intense mid-IR above-band-gap excitation at very short pump-probe delays $(t_D \approx 0)$ is of great interest both for computing the temporal evolution of picosecond Er^{3+} laser pulses within a resonator when ultrathin InAs epilayers are used as passive mode lockers and for studying the fundamental processes of carrier-carrier and carrier-lattice interactions. Although much experimental and theoretical effort has been devoted in the last decade to the investigation of the femtosecond dynamics of carriers in the wide-gap semiconductors GaAs and Al$_x$Ga$_{1-x}$As,[10–18] we are unaware of any similar studies in InAs and for our physical picture we rely on parallels with GaAs and Al$_x$Ga$_{1-x}$As experimental data for the typical carrier densities $(n \approx 1 \times 10^{17}$ cm$^{-3})$ used in our experiment (Table I).

Under intense pumping interband carrier excitation occurs over a continuum of states in the valence and conduction bands, the widths of which are determined by the inverse of the carrier dephasing time, if the spectrum of

the exciting pulse is narrow enough. The strongly modified carrier occupation statistics can then be studied by their effect on the small-signal absorption spectrum. Rapid scattering of carriers out of the initially excited narrow distribution occurs due to carrier-carrier or carrier-phonon scattering and in GaAs electron and hole quasi-Fermi distributions are typically established in a thermalization time scale T_1 of ≈ 100 fs, although at these early times the temperatures of the electron and hole quasi-Fermi distributions (T_e, T_h) may be substantially different.[17]

Phonon scattering then cools these Fermi distributions towards the lattice temperature on a picosecond time scale with overall absorption recovery occurring on time scales of the order of the carrier recombination time (100–1000 psec). For InAs the 77-fold difference between electron and hole densities of states means that in our experimental regime electron distributions are typically highly degenerate once the electron quasi-Fermi distribution is established (in contrast to the holes where the peak occupation factor rarely exceeds 0.1) and therefore dominate the absorption changes occurring due to band filling.

Undoped $d = 3.3$ μm thick InAs epilayers grown by molecular-beam epitaxy on GaAs substrates[5,8] are studied here at 300 K. A double-resonance infrared pi-

TABLE I. Typical carrier relaxation time constant in III-V polar semiconductors at $n_e \approx 10^{17}$ cm^{-3}.

Process	Time constant	Ref.
Carrier-dephasing T_2	45 fsec GaAs	12
Carrier thermalization, T_1	30–300 fsec GaAs Al$_x$Ga$_{1-x}$As	10–11 13–16
Carrier-lattice cooling	1–10 psec GaAs	13,16,17
Recombination time	35–3000 psec InAs	5,8
Radiative time	2.8 nsec InAs	5

cosecond spectrometer based on $LiNbO_3$ parametric superradiant generators pumped by a Nd^{3+}:YAG (yttrium aluminum garnet) laser[7] was used for the pump-probe studies and produced pump and probe pulses with full width at half maximum (FWHM) durations of 12 ± 2 psec which were independently tunable in the range $2700-3900$ cm^{-1} ($0.335-0.484$ eV) at a repetition rate of 50 Hz. To avoid interference effects and surface reflection losses all pump-probe measurements were performed at the InAs Brewster angle ($73.5°$). The pump pulse had an energy of 20 μJ and spot area 6 mm^2 giving a peak pump intensity in the sample of $I_{PU}=10^7$ W/cm^2. The probe pulse energy was 40 nJ over a 0.4-mm^2 spot. The angle between the beams was $13.5°$; both were polarized in the plane of incidence and had measured spectral widths of $10-20$ cm^{-1}.

In Fig. 1(a) the dynamic difference spectrum (DDS) [i.e., $\ln(T/T_0)$], is plotted as a function of probe photon energy at a fixed delay, where T_0 and T are the transmission values of the unperturbed and excited sample, respectively, and the excited carrier density is $(1-3)\times10^{17}$ cm^{-3}. At time delays ($t_D>15$ psec) the DDS curves closely follow (to within $<2\%$) the quasi-Fermi curves calculated assuming $T_e=T_h=300$ K. We use a parabolic three-band model to fit the absorption spectra with the (equal) electron and hole concentrations as the only fitting parameter. Band-gap renormalization (BGR) effects are neglected as the BGR shifts in the band energies are negligible compared with the Moss-Burstein absorption shift.[8]

The absence of a carrier temperature increase above the lattice temperature after the pump pulse has vanished is in agreement with our numerical modeling[19] of the deformation potential scattering energy loss rates which indicate that for these carrier concentrations the average carrier temperatures approach the lattice temperature to within 2% in less than 3 psec [similar to the GaAs case (Table I)]. The total pump energy absorbed by the sample during each pump pulse would result in a peak lattice temperature increase of the InAs of only 0.02 K per pulse.

Figure 1(b) shows the DDS at very early stages of excitation ($t_D\approx0$) when the calculated carrier density was $\approx10^{17}$ cm^{-3}. An obvious deviation from a quasi-Fermi distribution is seen, reaching its maximum at $t_D=0$. It consists of a sharp spike about 20 cm^{-1} wide centered on the pump frequency ($h\nu_{PU}$) and superimposed on a broader feature which spreads some hundreds of cm^{-1}. The central sharp spike is a "coherence artifact" (CA)— it occurs due to parametric coupling between the pump and probe beams by an index grating produced by the spatially varying electron-hole plasma distribution.[20] The CA occurs only when the pump and probe pulses coincide in both frequency and time and carries no information about carrier dynamics. For crossed pump and probe polarizations the CA disappears in our experiment but this geometry cannot be used over a large probe frequency range here because the resulting nonzero reflectivities give strong Fabry-Pérot fringes which distort the DDS spectra.

We attribute the broader feature in the DDS above the

quasi-Fermi function line to the existence of nonthermalized electrons. The above-Fermi distribution (revealing itself as a spectral hole in the sample transmission) follows in its amplitude the instantaneous pump intensity and disappears when the pump pulse vanishes. It is centered at the spectral position of the pump beam and closely follows changes in $h\nu_{PU}$ (Fig. 2), over a range of ±100 cm^{-1}. In contrast to previous studies[11] these spectral holes are created in a quasi-steady-state regime; the pump and probe pulses are both more than 50 times longer than reasonable T_1 and T_2 values and the spectral holes appear due to a dynamic balance between carrier creation by intense interband excitation on the one hand and carrier scattering out of the initial photoexcited states by the thermalization processes (described by T_1) on the other.

The difference spectra between the nonequilibrium DDS, normalized to the small-signal absorption, are plotted in Fig. 3. For a simple two-band model the change in the absorption coefficient $\alpha(\omega)$ depends on the changes in the electron (f_e) and hole (f_h) occupation factors of the states optically coupled to the light at frequency ω as $\alpha(\hbar\omega)=\alpha_0(\hbar\omega)(1-f_e-f_h)$. In the (reflectionless) Brewster geometry the optical density is

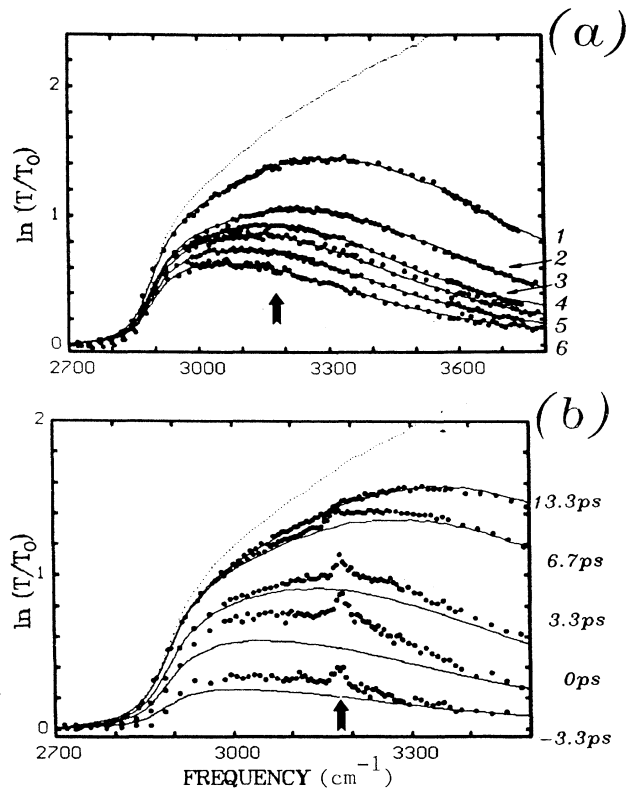FIG. 1. Dynamic difference spectra at fixed delay and 3180-cm^{-1} pump frequency. (a) Case of large delays: 1, $t_D=20$ psec; 2, 620 psec; 3, 890 psec; 4, 1.02 nsec; 5, 1.55 nsec; 6, -2.09 nsec. (b) At early stages of excitation. Solid curves, calculated absorption assuming quasi-Fermi distributions with $T_e=T_h=300$ K. Dotted curves, small signal absorption ($\alpha_0 d$) taken with a Fourier spectrometer. Arrows show the position of the pump frequency.

$D(\hbar\omega)=\alpha(\hbar\omega)d=-\ln(T)$, hence $D=D_0(1-f_e-f_h)$. We measure $\ln(T/T_0)=D_0-D$, and define the quantity $f\equiv(D_0-D)/D_0=[\ln(T/T_0)]/D_0=f_e+f_h$ as being the sum of the changes in the occupation probabilities in the conduction and valence bands. In the case of a three-band semiconductor the situation is slightly more complicated because the same photon couples transitions from hh and lh (light-hole) bands to the conduction band but the quantity f still has the physical sense of an occupancy change (Fig. 3).

The spectral holes have typical widths of 300 cm^{-1} and amplitudes corresponding to a maximum occupation probability change[23] of $f=0.1-0.15$. Their forms are slightly asymmetric: for $t_D<0$ they appear at lower energies [Fig. 3(a)] because the carriers are mainly scattered to lower energies from their initial photoexcited states. At later instants the scattering to lower energies slows as the lower conduction-band states begin to fill and block intraband scattering processes. Similar effects are seen in the spectral dependence at $t_D=0$ [Fig. 3(b)]: at higher $h\nu_{PU}$ the carriers are scattered preferentially to lower energies while at lower $h\nu_{PU}$ the states with smaller energies are already partially occupied during the pump pulse.

This effect of energy redistribution to higher-energy states is indirect evidence that carrier-carrier scattering plays at least a comparable role in the initial carrier re-laxation processes to that of carrier-phonon scattering. In the latter case a net energy loss to the lattice is expected. Another possible source of the observed asymmetry in the spectral hole is the three-band nature of the InAs band structure. Electron states filled by e-hh band transitions produce a decrease of the e-lh band absorption at a higher photon energy and vice versa. The e-lh absorption however is weaker by a factor of 0.43 (Ref. 8) and the saturation of its absorption due to band filling starts earlier.

To analyze our results we use the rate equation treatment of Ref. 10, adapting it to the quasi-steady-state case. This approach is also very similar to that used in Refs. 21 and 22 to analyze the hole-burning effect for intervalence-band transitions in p-type germanium. The band-to-band transitions are treated as being due to excitation of an ensemble of two-level systems with an energy separation $\hbar\omega$ and a density of states $\rho(\hbar\omega)$ where $\rho(\hbar\omega)=(2\pi^2)^{-1}(2\mu^*/\hbar^2)^{3/2}(\hbar\omega-E_g)^{1/2}$ and $\mu^{*-1}=m_e^{*-1}+m_{hh}^{*-1}$. The homogeneous linewidth of each individual transition is $\Gamma=1/T_2$ and T_1 corresponds to the relaxation time of the nonthermalized carrier population [described by a probability distribution $f(t,\hbar\omega)$] towards a thermalized distribution between the ensemble of two-level systems. This definition of T_1 amounts to a considerable simplification of what is in reality a rather
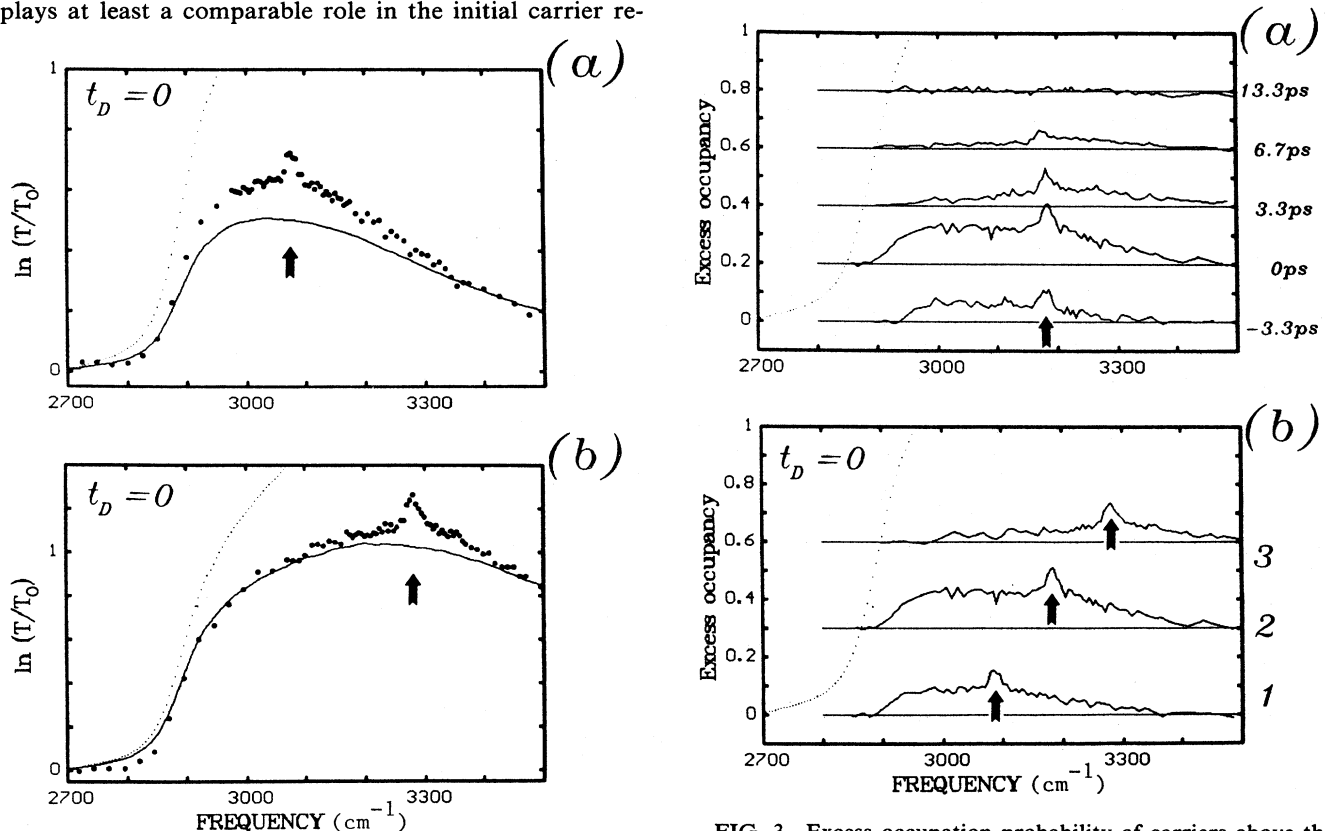

FIG. 2. Dynamic difference spectra at $t_D=0$. (a) 3080-cm^{-1} pump photon frequency. (b) 3280-cm^{-1} pump photon frequency, Solid curves correspond to quasi-Fermi distributions with $T_e=T_h=300$ K. Dotted curve-small signal absorption. Arrows show the position of the pump frequency.

FIG. 3. Excess occupation probability of carriers above the quasi-Fermi distribution, f_{nt}. (a) At 3180-cm^{-1} pump frequency and different pump-probe time delays. (b) At $t_D=0$; 1, pump frequency 3080 cm^{-1}; 2, 3180 cm^{-1}; 3, 3280 cm^1. Dotted curve, small signal absorption. Arrows show the position of the pump frequency. Successive plots vertically shifted for clarity.

complex many-body scattering process. More strictly the effective "relaxation time" is a function of the carrier energies within the nonthermalized part of the distribution, but the ensuing analysis is sufficient to provide an estimate of the relevant time scales.

The occupation probability function $f(t,\hbar\omega)$ is modeled as a sum of a thermal distribution $f_{th}(t,\hbar\omega)$ and a nonthermal one $f_{nt}(t,\hbar\omega)$. The rate equation for $f_{nt}(t,\hbar\omega)$ is thus

$$(d/dt)f_{nt}(t,\hbar\omega) = \Omega^2[1-f(t,\hbar\omega)]\Gamma/[(\omega-\omega_p)^2+\Gamma^2]$$
$$-f_{nt}(t,\hbar\omega)/T_1 , \qquad (1)$$

where $\Omega=\mu E_0/\hbar$ is the Rabi frequency, μ the interband matrix transition element, E_0 the amplitude of the optical field, and ω_p the pump photon frequency.

In the steady state Eq. (1) can be solved for f_{nt} giving

$$f_{nt}(\hbar\omega) = [1-f(\hbar\omega)]I/\{1+I+[(\omega-\omega_p)^2/\Gamma^2]\} , \qquad (2)$$

where $I=\Omega^2 T_1 T_2$ is the light intensity I_{PU} normalized to the saturation intensity I_s, where

$$I_s = [\pi\hbar^2\omega\rho(\hbar\omega)]/[2\alpha_0(\hbar\omega)T_1 T_2] . \qquad (3)$$

At $t_D=0$ and $\omega\approx\omega_p$ [Fig. 3(a)] we measure the hole depth (after deducting the CA peak) to give $f_{nt}\approx 0.17$ (Ref. 23) and $f=0.42$. So we find from (2) that $I\approx 0.41$ in our experiment. From the known value of the pump intensity $I_{PU}=10^7$ W/cm^{-2} we calculate that $I_s=2.41\times10^7$ W cm^{-2}. Using the values $m_e^*=0.022m_0$, $m_{hh}^*=0.4$,[1] and the measured $\alpha_0(\hbar\omega)=4.85\times10^5$ m^{-1} at $\hbar\omega=0.394$ eV (Ref. 8) in Eq. (3) we calculate

$$T_1 T_2 = 2.40\times10^{-27} \text{ sec}^2 . \qquad (4)$$

On the other hand, from Eq. (2) it follows that the hole spectral width (FWHM) is $\Delta\nu=(1+I)^{1/2}(\pi T_2)$; taking

the experimental value of $\Delta\nu=340$ cm^{-1}, we get $T_2=37$ fsec and from (4) $T_1=65$ fsec.

The accuracy of T_1 and T_2 values is estimated to be no better than $\pm40\%$ taking into account the difficulties of measuring I_{PU} on the sample and the simplifying assumptions of the model (e.g., the assumption of a constant T_1 and f_{th} over the width of the spectral hole). The model used here is also too simple to account for the asymmetric form of the hole burned. The measured T_1 and T_2 values are nevertheless of the same order of magnitude as the GaAs and $Al_xGa_{1-x}As$ data presented in Table I.

From the above analysis, however, we cannot specify whether the scattering process is dominated by electrons or holes, because their role in the absorption change due to state filling is equivalent. We note only that for the holes higher scattering rates from the initial state after optical excitation are expected because the holes are always nondegenerate at 300 K at these carrier densities, in contrast to the strongly degenerate electron gas.

The ultrafast bleaching component associated with nonthermalized carriers may be important for Er^{3+} laser switching applications, and may allow gain-transform limited pulsed laser operation, similar to recently reported[24] results where a KCl:Li color center laser/$Hg_{1-x}Cd_xTe$ multiple-quantum-well combination produced 120-fsec pulses near $\lambda=2.8$ μm. In InAs we estimate that for typical Er^{3+} cavity parameters the fast nonthermalized bleaching will dominate over the slower band-filling component for laser pulse durations < 10 psec.

*Permanent address: General Physics Institute, Vavilov str.38, Moscow 117942, Russia.

[1]Numerical Data and Functional Relationships in Science and Technology, Landolt-Börnstein, New Series, Group III, Vol. 22, Pt. a (Springer, Berlin, 1987), pp. 117 and 118.

[2]C. D. Poole and E. Garmire, Appl. Phys. Lett. 44, 363 (1984).

[3]C. D. Poole and E. Garmire, IEEE J. Quantum. Electron. QE-21, 1370 (1985).

[4]V. I. Kovalev et al., Infrared Phys. 31, 343 (1991).

[5]C. C. Phillips, et al., J. Phys. D 24, 437 (1991).

[6]K. L. Vodopyanov et al., Appl. Phys. Lett. 59, 1658 (1991).

[7]H. Graener et al., Chem. Phys. Lett. 140, 306 (1987).

[8]K. L. Vodopyanov et al., Phys. Rev. B 46, 13 194 (1992).

[9]K. L. Vodopyanov et al., J. Appl. Phys. 73, 1 (1993).

[10]J. L. Oudar et al., Phys. Rev. Lett. 55, 2074 (1985).

[11]W. H. Knox et al., Phys. Rev. Lett. 56, 1191 (1986).

[12]P. C. Becker et al., Phys. Rev. Lett. 61, 1647 (1988).

[13]See, e.g., D. von der Linde, in Utrashort Laser Pulses and Applications, edited by W. Kaiser, Spring Topics in Applied Physics Vol. 60 (Springer, Berlin, 1988), and references therein.

[14]W.-Z. Lin et al., IEEE J. Quantum Electron. QE-24, 267 (1988).

[15]J. Nunnekamp et al., Phys. Rev. B 43, 14047 (1990); T. Elsaesser et al., Phys. Rev. Lett. 66, 1757 (1991).

[16]D. W. Snoke et al., Phys. Rev. Lett. 68, 990 (1992).

[17]C. W. W. Bradley et al., Solid State Electron. 32, 1173 (1989).

[18]J.-P. Foing et al., Phys. Rev. Lett. 68, 110 (1992).

[19]Carrier energy loss rates were computed by taking experimentally measured carrier distributions and integrating the expressions in Sec. 3.5 of B. K. Ridley, Quantum Processes in Semiconductors (Clarendon Press, Oxford, 1988), pp. 269-276.

[20]C. V. Shank and D. K. Auston, Phys. Rev. Lett. 34, 479 (1975).

[21]F. Keilmann, Appl. Phys. 14, 29 (1977).

[22]R. Till and F. Keilman, Phys. Rev. B 44, 1554 (1990).

[23]Here we have taken the depth of the spectral hole to be $\sqrt{2}$ times larger than is directly measured from Fig. 3. This is because the pump and probe pulses have the same temporal profile and, as the spectral hole depth follows the pump intensity temporal profile, the observed effect is the convolution of the two pulses.

[24]C. L. Cesar et al., in Utrafast Phenomena VII, edited by C. B. Harris et al. (Springer, Berlin, 1990), p. 17.